Induced Radioactivity

Max Christopher* and Xiaoyuan Zhang†
Department of Physics, Harvard University, Cambridge, MA 02138

We measured the half-lives and energy spectra of aluminum, silver, copper and indium foils that were activated in a neutron moderator. The half-lives we obtained are in good agreement with the literature values. These properties allowed us to identify unknown samples. Then, we found that cadmium shields silver's lighter stable isotope from being irradiated by free neutrons in the neutron moderator. We also discovered that the initial count of irradiated silver atoms in the sample appears to increase exponentially with irradiation time until it reaches its saturation point.

I. INTRODUCTION

A. Radioactive Decay

1 Radioactivity is the process by which an unstable atomic nucleus loses energy. This phenomenon is found naturally within the isotopes of certain elements and was first discovered in phosphorescent materials studied by Henri Becquerel and Marie Curie in 1896 [1, 2].

2 The process in which the nuclei of unstable atoms return to a more stable state is called radioactive decay. A radioactive material obtains this more stable state as it loses energy by emitting particles or photons. The three major decay types are denoted α, β and γ decays. An α-decay is when an unstable isotope's nucleus loses two neutrons and two protons in the form of a helium atom. Therefore, α-particles have a positive charge of 2+ [3]. In a β-decay, a neutron turns into a proton, and emits an electron and a neutrino. Therefore, β particles carry a negative charge [3]. Finally, there are also γ-decays, which is radiation released from an excited state as light. This means that the nucleus releases a photon [3]. No matter the form of decay, an unstable isotope must release energy in order to return to a more stable state.

3 For a given unstable isotope, the probability that it will decay in any time interval is constant. Therefore, the rate of decays, dN/dt, is proportional to the total number of unstable isotopes N with some proportionality constant λ [3, 4]:

$$\frac{dN}{dt} = -\lambda N. \tag{1}$$

Here, λ is defined as the decay constant and is characteristic to the radioactive isotope. We solve this differential equation to arrive at the radioactive decay law

$$N(t) = N_0 e^{-\lambda t} = N_0 e^{-t/\tau} \tag{2}$$

where N_0 is the initial quantity of radioactive material [3]. Also notice that $\tau \equiv 1/\lambda$ where τ is called the mean lifetime. This function allows us to determine the number of radioactive particles present in the sample at time t. This solution shows that radioactive decay is exponential: the more activated radionucleotides present a particular sample, the more decays will occur in a given time [3].

4 The exponential decay equation becomes even more intuitive when we introduce the half-life, $t_{1/2}$. This variable represents the time required for half of the radionuclide's atoms to decay [3]. With the radioactive decay law in this form, if a sample starts with N_0 radioactive particles, then after a single half-life there will be $N_0/2$ radioactive particles in the same sample. After another half-life, there will be $N_0/4$ radioactive particles. Explicitly, the half-life equation is [3]

$$N(t) = N_0 \left(\frac{1}{2}\right)^{t/t_{1/2}}. \tag{3}$$

We can determine $t_{1/2}$ directly from our previous equations. Letting $t = t_{1/2}$ in Eq. (2) and Eq. (3), we can set them equal and solve for $t_{1/2}$ to find that

$$t_{1/2} = \tau \ln 2. \tag{4}$$

By convention, we will use the half-life decay model throughout this paper to measure radioactive decay.

B. Induced Radioactivity

5 Induced radioactivity refers to the process of activating a stable material using radiation. This means that we are putting a stable isotope into an unstable state in which it will then radioactively decay. One form of induced radioactivity is photodisintegration, where the nucleus loses a neutron when hit by a high energy photon [5]. However, unstable isotopes can also be created through a process called neutron activation. Neutron activation is a form of induced radioactivity in which an atom becomes a heavier isotope by capturing one or more free neutrons from a neutron moderator. If the product isotope resulting from the nucleus of the atom gaining an additional neutron is an unstable product, the newly radioactive product will immediately begin to decay. The half-lives of these decays are entirely dependent upon their elemental isotope [6].

* maxwellchristopher@college.harvard.edu
† xiaoyuanzhang@g.harvard.edu

6 In order to determine the formula for induced radioactivity, we need to understand the relationship between irradiation time and neutron cross sections. An element's irradiation time refers to the amount of time it takes for the sample to become saturated with radioactive particles when exposed to a neutron moderator. This can effectively be thought of as how quickly the sample will become radioactive. An element's neutron cross section, σ, is a value that expresses the probability of a free neutron interacting with that element's nucleus and is measured in m^2. It can be used with neutron flux in order to determine the irradiation time [7]. However, as soon as a particle becomes irradiated, it begins to decay. Thus, we can determine the rate of irradiation, dn/dt, using the equation

$$\frac{dn}{dt} = \frac{\sigma}{b}(N - n) - \frac{n}{\tau} \tag{5}$$

where N is the total molecules, n is the radioactive molecules (which means that $N - n$ are the inactivate molecules), and b is some constant. Solving this equation shows that the irradiation rate increases with increasing cross sections exponentially:

$$n(t) = \frac{N\sigma\tau}{b + \sigma\tau} + c_1 e^{-\left(\frac{\sigma}{b} + \frac{1}{\tau}\right)t} \tag{6}$$

and the initial count after a irradiation time T is

$$N_0 \equiv n(T) - n(0) = c_1 \left(e^{-\left(\frac{\sigma}{b} + \frac{1}{\tau}\right)T} - 1\right) \tag{7}$$

Here c_1 is another constant from the differential equation.

C. Energy Spectra

7 Neutrons undergoing radioactive decay emit can emit gamma rays if in γ-decay. These electromagnetic waves have various intensities and energies and are different depending on the radioactive materials [8]. Therefore, if a spectrum of energies is measured from a particular radioactive source, it will create a fingerprint of energy peaks at certain distinctive values for that material.

D. Experimental Motivation

8 Here we use a neutron moderator to induce radioactivity in a variety of metal foils and investigate multiple associated properties. We reproduce standard values for half-life decays using a standard Geiger counter and create reproducible energy spectra for their radioactive energy. These spectra allow us to identify unknown irradiated elements by comparing them to the peaks of the identified elements. We also explore the shielding properties of cadmium, finding that it preferentially blocks the irradiation of Silver-107, while allowing Silver-109 to be irradiated relatively unopposed. Finally, we determined the initial count of irradiated material increases as we increase the irradiation time of silver until the sample reaches its saturation point.

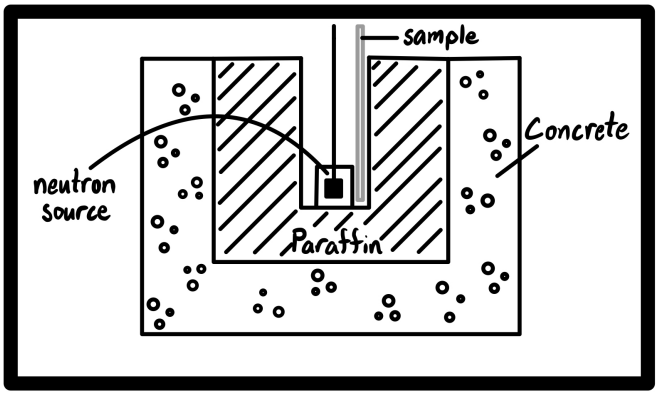

FIG. 1. A diagram of the neutron moderator used for irradiating the metal foils. The metal foils were attached at the end of the rod labeled 'sample' in order to be as close as possible to the neutron source.

II. EXPERIMENT SETUP

A. Apparatus

9 The neutron moderator is the mechanism in which free neutrons are created to be captured by the nuclei of elemental samples. We use a neutron moderator consisting of a 239Pu-Be neutron source within a large concrete enclosure filled with paraffin. See Fig. 1 for diagram of the neutron moderator. Neutrons are created by the neutron source as Pu-239 decays and its α-particles mix with Be-9. This reaction emits high energy neutrons that are absorbed by the surrounding paraffin (hydrocarbon mixture). Initially, the free neutrons are extremely fast with energies in the range of $1 - 11$ MeV, but as the neutrons collide with the paraffin, they lose energy rapidly [9]. This energy loss occurs because the free neutrons are of about equal mass to the hydrogen atoms in the paraffin. This ensures the neutrons slow to an ideal energy to be captured by metal foils inserted into the moderator [10]. Samples to be activated are taped to the end of a long plastic rod that can be placed inside the neutron moderator. The rods can be accessed and transported to the testing site using long tongs where the sample can then be removed and used for experimentation.

10 Once a sample is activated in the neutron moderator, we can measure its half-life using a Geiger counter. The sample is placed inside of a lead cylinder on wheels in order to shield the outside environment from radiation and protect the Geiger counter from cosmic rays and other background signals. Then the tube is rolled into place so that the activated sample is aligned with

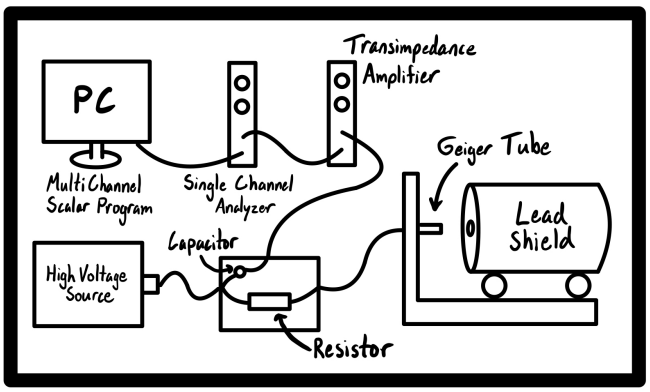

FIG. 2. A diagram of the apparatus used for measurement using the Geiger counter. The radioactive sample is placed in the Geiger counter lead shield. After running the high voltage through the Geiger tube, the output signal is passed to the MCS Program on the computer.

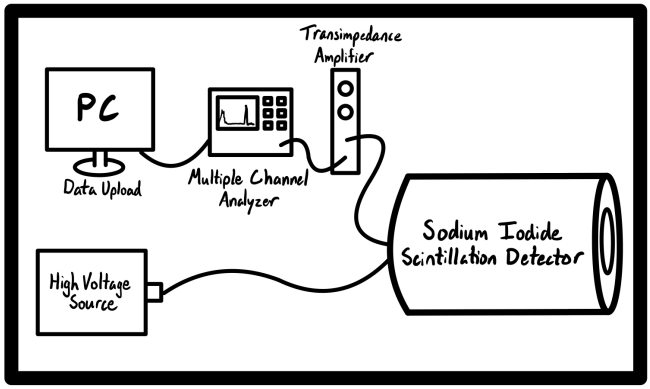

FIG. 3. A diagram of the apparatus used for measurement of energy spectra with the sodium iodide scintillation detector. The radioactive sample is placed within the detector's lead shield. Once the signal is passed to the MCA, the data can be uploaded to the computer for analysis.

the Geiger counter. The Geiger counter is a tube that converts radiation into electrical signals. It consists of a metal cylinder with a wire running down its center [11]. Our counter is filled with a noble gas at partial pressure (although the manufacturer does not release these exact specifications, it is a Victoreen VG-41 Geiger tube). When a high voltage is passed through the device, the gas is ionized. Through our calibration, we determined that the ideal voltage to run through the Geiger tube was 510 Volts (see Appendix 1 for the detailed calibration procedure). The high voltage must be passed to the Geiger counter through a series resistor (1 million Ohms) to limit current and a parallel capacitor (180 picofarads) to extract the signal pulses. As particles pass through the Geiger tube, they set off chain reactions of ion pulses which can be detected and recorded. These pulses can be initiated by α, β and γ particles [11]. This signal is then passed from the Geiger counter to a transimpedance amplifier, which increases the voltage of the signal, and then to a single channel analyzer, that converts the analog pulses into constant logic pulses. Finally, the signal is transmitted to a MultiChannel Scalar (MCS) software. The MCS records the number of counts registered over a certain amount of time, binning the data into a chosen time interval, which then can be used to calculate rates of decay. A schematic diagram of the equipment used in this experiment is shown in Fig. 2.

11 In order to measure the energy spectra of the activated samples, we used a sodium iodide scintillation detector. This detector is shielded by a large lead cylinder with an opening for the samples to be placed inside. The detector itself is composed of a cylindrical thallium doped sodium iodide (NaI(Tl)) scintillation crystal coupled to a photomultiplier tube. These components are inside in an aluminum container. When a radioactive sample is placed near the detector, any gamma-rays that enter the NaI(Tl) scintillation crystal will lose energy due to Compton scattering within the crystal. These scattering events produce light that can be detected by the photomultiplier tube [8]. The detector measures on channels of voltages ranging from 1-1200. This signal is then sent to the multiple channel analyzer (MCA) which records counts per channel, producing a range of peaks at different channels, representing energy values of the samples. Therefore, these channels must be calibrated with their corresponding energy values (see Appendix 2 for our calibration procedure). See Fig. 3 for a diagram of the equipment setup.

B. Experiment Procedure

12 We collected data to measure the half-lives of silver (Ag), copper (Cu), aluminum (Al) and indium (In). Before activating our samples in the neutron moderator, we had to estimate their activation times. To do so, we checked the table of nuclides to determine the expected half-lives of each sample. Because the neutron moderator would add one neutron to the nuclei of our foils, we checked the chart for the stable isotope(s) of each element tested and located the isotopes with one additional neutron. Using the half-lives recorded here, we estimated that we had to irradiate the foils for at least 4 to 5 times their half-life (or longest half-life) to reach the saturation point. The accepted values can be seen in Table I. With our irradiation times determined for each element, we activated our samples in the neutron moderator and brought them to the Geiger counter for measurement. For each sample, we collected the number of counts in 1 second intervals for multiple half-lives of the element. For silver, copper and aluminum, we found it sufficient to record decay rates for 900 seconds (or 15 minutes). At this time interval, counts were reduced to noise by the end of data collection. For indium, we increased our time of measurement since the longer decay of Indium-117 was also observed. Because the half-life of Indium-

116 is so short, it is very unlikely that any of this isotope was present to begin with. This means that the stable isotope, Indium-115 must have captured 2 free neutrons. Therefore we increased our irradiation time for indium and measured its decay with the Geiger counter for 2100 seconds (or 35 minutes). We repeated this process and collected 5 data sets for each of our 4 elements.

Metal Foil	Radioactive Isotopes	Half-Life (Seconds)
Aluminum (Al)	Al28	134.40
Copper (Cu)	Cu64	45723.60
	Cu66	306.00
Silver (Ag)	Ag108	143.40
	Ag110	24.60
Indium (In)	In114	71.88
	In116	14.10
	In117*	2640.00

TABLE I. The expected isotopes and half-lives of our irradiated metal foils based on the chart of nuclides [12]. *In117 would have needed to capture 2 free neutrons to be present in our sample, but our data reflects that this isotope may have been present in our sample.

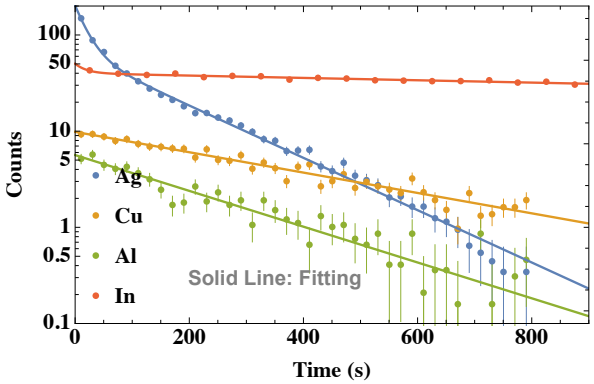

FIG. 4. The exponential decays of activated samples in a log-linear plot. The points represent the experimental data and their associated error while the solid curves are the exponential curve fits for the data. We subtracted the constant term, B, in both the data and the fitting curves. Note that the indium and silver have two decay modes. See Fig. 5 for a zoom-in plot for indium.

13 We used the sodium iodide detector to measure the energy spectra of our test samples: indium, copper, aluminum and silver. After irradiating the samples in the neutron moderator for 4-5 of their half-lives, we put the activated samples in the sodium iodide detector to collect their gamma spectrum data. This data was recorded in counts per energy level. We measured the irradiated element samples for differing times due to their varying half-lives. Therefore, we normalized the data to the count rate (counts per second) per energy level. Finally, to eliminate false background peaks, we subtracted the background fit function, Eq. (13), determined in the calibration procedure from our data for each sample (refer to Appendix 2 for details). This resulted in a unique energy spectrum with characteristic peaks for each element. In order to determine the position of the peaks for each normalized (and background-removed) spectrum, we fit them with the Breit–Wigner distribution [13, 14] detailed in Eq. (12) (see the details in Appendix 2). The location parameter was then determined to be the position of the peak. By repeating the measurement of the peak for multiple data sets, we can calculate the average and the standard deviation of peak position [15]. By evaluating the position of the resulting peaks with respect to the calibrated energy channels, we determined the corresponding energy values for each sample. The final results and energy values are shown in Section III.

III. EXPERIMENTAL RESULTS

A. Half-Lives of Activated Samples

14 As expected, our data represents an exponential decay model. By measuring the count rate with respect to time, we can easily see that the evolution of all samples exhibit one or two exponential behaviors. This characteristic can be seen in Fig. 4 and 5, where we show the exponential curve fits to our experimental data. In the figure, the initial count values vary for different samples since their neutron cross sections are not identical (neutron cross section values are listed in Table III). The activation time also could affect the initial count rate. If not irradiated for long enough, it may not reach the saturation point for the sample. Since this is a counting experiment, we use the standard deviation of Poisson distribution, $\sqrt{N}$, to estimate the error. Also, when binning the data, we propagate the error to the new data sets. In both Fig. 4 and 5, we bin the data into 20 second intervals for silver, copper and aluminum, and 50 second intervals for indium.

15 From the exponential decays, we calculated the half-lives of each element isotope tested. From Table I, we learn that some materials have two decay modes, and thus we use a double-exponential function to fit the data:

$$N(t) = N_1 e^{-t/\tau_1} + N_2 e^{-t/\tau_2} + B \tag{8}$$

where $\tau_1 \ln 2$ and $\tau_2 \ln 2$ will be the half-lives of two decay mode, N_1 and N_2 are the initial number of particles and the constant fit parameter B stands for the background radiation. For those with one possible decay mode, we use the single exponential function instead.

$$N(t) = N_1 e^{-t/\tau_1} + B \tag{9}$$

In this letter, we use the built-in functions `FindFit` in `Mathematica`. The fitting lines are also shown in Fig. 4 and 5. Then for each sample, we repeat the experiments several times and perform the exponential fitting to determine the half-lives. Eventually, we use the average of

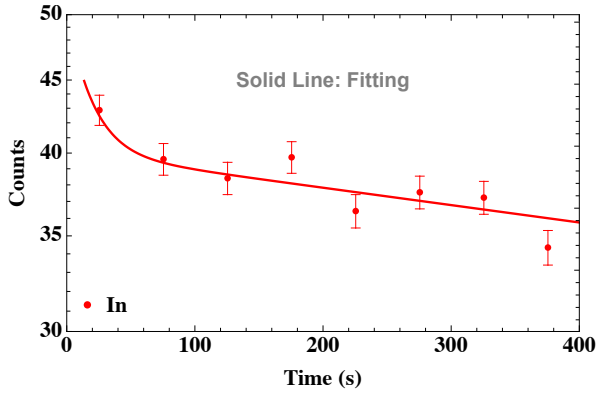

FIG. 5. The exponential decays of activated indium in a log-linear plot. The points represent the experimental data and their associated error while the solid curves are the double exponential curve fits for the data. We subtracted the constant term, B, in both the data and the fitting curves.

all test results as the half-lives for each element and estimate the error with the standard deviation. Our results for silver, copper, aluminum and indium are summarized in Table II.

Sample	Experiment Value (second)	Standard Value (second)	Error Percentage
Aluminum (Al) 128	152.44 ± 8.00	134.40	13.43%
Copper (Cu) 66	325.94 ± 26.54	306.00	6.52%
Silver (Ag) 108	143.97 ± 9.17	143.40	0.40%
Silver (Ag) 110	23.88± 2.32	24.60	2.92%
Indium (In) 116	11.57 ± 1.92	14.10	18.00 %
Indium (In) 117	2841.97 ± 368.37	2640.00	7.70%

TABLE II. Half-lives of silver, copper, aluminum and indium. The second column is our experiment data, with the error estimation for repeated measurement. The third column is the value from literature. The last column is the deviation between experiment data and standard values.

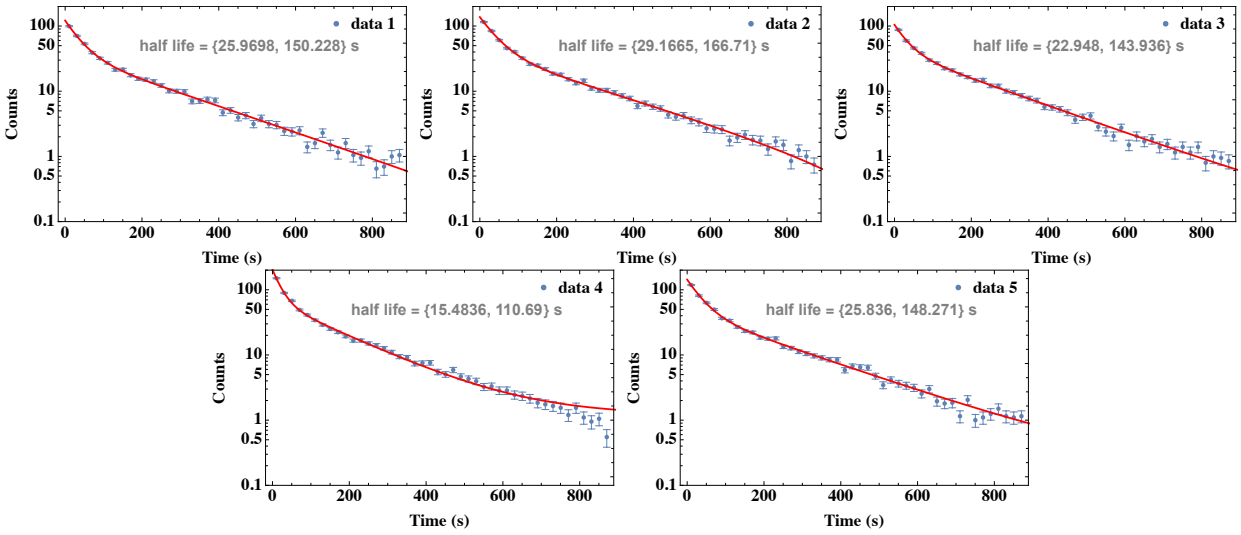

FIG. 6. Detailed data for the half-life measurements of silver. Each plot represents one measurement and its exponential fitting using Eq. (8). Again the error is estimated using Poisson distribution. Note that we didn't subtract the constant term B in the figures.

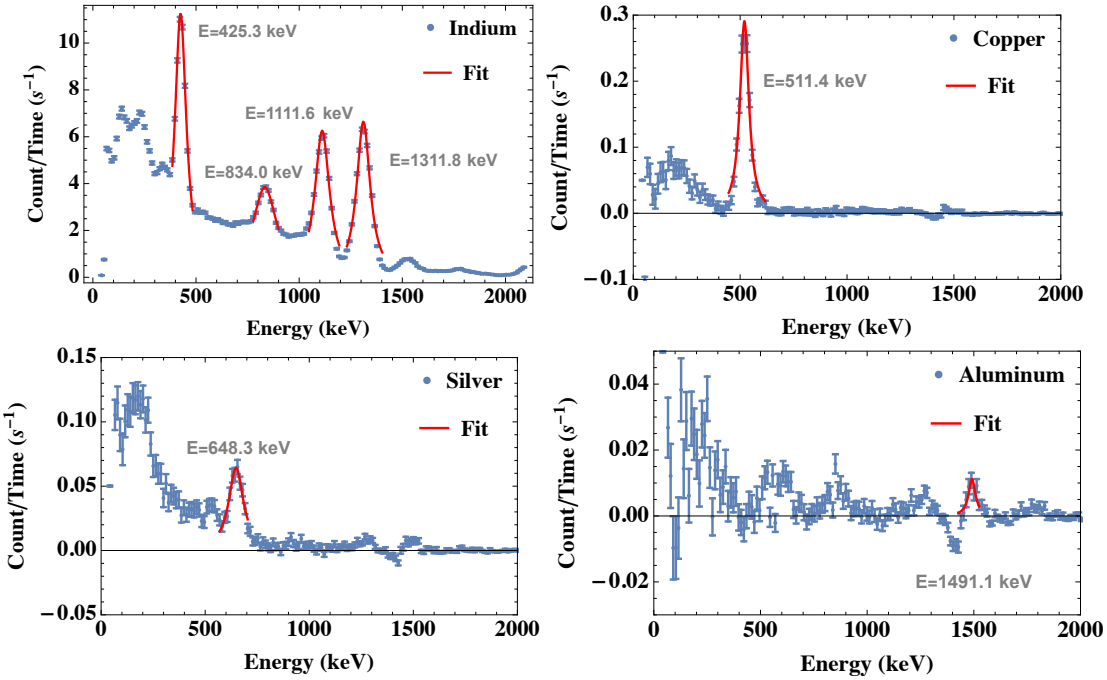

FIG. 7. The energy spectrum of activated samples. The blue points are from experimental data, with the error estimated by Poisson statistics. The red solid lines represent the peaks that are found by Breit–Wigner distribution locally.

16 Among all the tested materials, silver exhibits the best behavior. The silver data appeared to be the most repeatable of our elements, and its half-life results most closely matched the literature values. In Fig. 6, we show the experimental data for all five measurements of silver's decay. Each data set clearly depicts both exponential decay modes. For each measurement, we fit the data using Eq. (8) and obtained the two half-lives. Then we calculated the half-lives by averaging the five measurements, and estimated the error with standard deviation. We used this same process to compute the half-lives of the other elements.

17 While many of our samples provided strong data, the aluminum data sets appeared very noisy due to their low initial count rate (as seen in Fig. 4). This resulted in a large error percentage for the measured half-life. This is likely due to aluminum's small neutron cross section (see Table III). Referring to Eq. 5, we know that a small cross section will lead to a very slow rate of irradiation. The expected unstable isotopes of aluminum have small neutron cross sections and short half-lives. In fact, it is possible that the rate of irradiation was so slow that even while constantly exposed to the neutron moderator, the isotopes decayed too quickly for the sample to remain strongly irradiated. This is a plausible explanation for the weak signal of the aluminum and explains the low initial count rate. In order to obtain a precise half-life, we may need a more sensitive detector. This is also consistent with our most active elements. As the relatively large cross sections of silver and indium would suggest (from Table III), these were the elements that gave us the largest initial counts.

Metal Foil	Stable Isotopes	Cross Section (Barns)
Aluminum (Al)	Al27	0.231 ± 0.003
Copper (Cu)	Cu63	4.50 ± 0.02
	Cu65	2.17 ± 0.02
Silver (Ag)	Ag107	34.8 ± 1.2
	Ag109	93.4 ± 0.6
Indium (In)	In113	12.0 ± 0.6
	In115	202 ± 2

TABLE III. The neutron cross sections of the stable isotopes of our experimental samples. These values were determined through the chart of the nucleotides [12].

B. Energy Spectra of Activated Samples

18 In this subsection, we will present the energy spectra for several activated samples. Fig. 7 shows the energy

spectra of all activated samples, including indium, copper, aluminum and silver. Since we subtracted the background using Eq. (13), both the low energy spectrum and the potassium peak are suppressed. Indium has the most peaks among all the measured activated samples. Using the relation from the calibration, we can identify their energies. The peaks are summarized in Table IV. We are unsure if our data reveals a true peak in the aluminum sample. The aluminum energy spectrum suggests that a peak may exist around 1491.08 keV. However, due to aluminum's low neutron cross section, this would require further investigation.

19 It is difficult to compare our experiment peaks with those in the literature. Indium has more than nine typical radiations from 158.6 keV to 1299.9 keV, and some of them are hard to distinguish. For example, two standard peaks are 1293.60 keV and 1299.90 keV, and thus what we measure could be a combination of peaks.

Sample	Peak Position (keV)
Indium	452.3 ± 0.1
	834.0 ± 0.4
	1111.6 ± 0.3
	1311.8 ± 0.5
Copper	511.4 ± 1.6
Silver	648.3 ± 6.3
Aluminum[a]	$1491.1\pm$

[a] Aluminum doesn't have a error since we don't have time to repeat the measurement.

TABLE IV. The peak positions of all samples. Indium has four peaks while the others only have one.

C. Identify Unknown Samples

20 We can use the characteristic half-lives and energy spectra of the elements to identify the identity of unknown samples. We had two unknown samples, labeled Unknown 1 and Unknown 5 that we tested for this experiment. We found that the small quantity of material to be irradiated made the half-life data from the Geiger counter very weak and noisy. This made it relatively impossible to fit an accurate curve to the data to determine the half-lives. Therefore, we had to rely on the measurements of the energy spectra of the unknown samples (see Fig. 8). From this data, Unknown 1 was easily identified as indium since its four peaks coincided with our measured values for our indium sample. However, for Unknown 5, we found three peaks in a pattern that did not match any of our identified data. This leads us to believe that Unknown 5 must not be one of the elements we have tested. With more time, and the opportunity to categorize energy spectrum for more elements, it is plausible that we could identify Unknown 5 from its energy spectrum alone. We also expect that with more active, or simply larger, unknown samples, it would certainly be feasible to deduce the identity of the unknown element through its characteristic half-life.

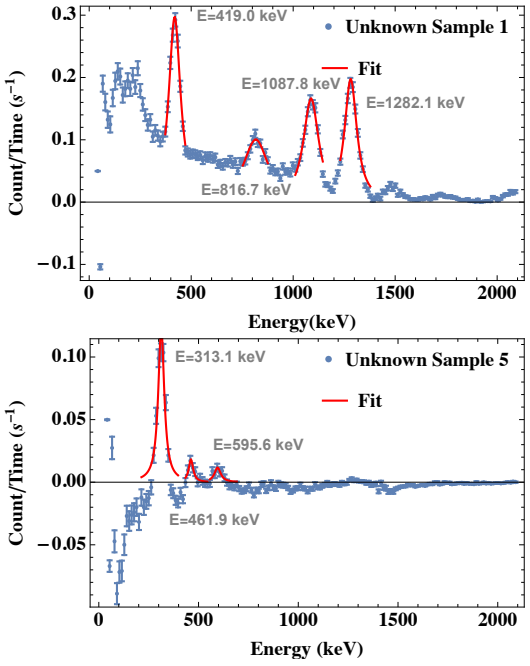

FIG. 8. The energy spectra from samples Unknown 1 and Unknown 5. Unknown 1's energy spectrum coincides with our identified indium spectrum.

D. Cadmium Neutron Shielding

21 Cadmium has certain shielding effects similar to the lead used in the radiation shields of other parts of our experiment. We irradiated silver sandwiched between cadmium foils to evaluate these shielding effects. While we were unable to completely encase the silver in a cadmium enclosure, most of the silver's surface area was shielded by the cadmium foil. We performed both the half-life and energy spectrum measurements with the cadmium shielded silver. The spectrum is shown in Fig. 9, which is effectively equatable to a background measurement. This means that the cadmium was at least shielding the activation of the isotope corresponding to the single peak in our unshielded silver energy spectrum data.

22 Next, we investigated the same cadmium shielded silver using the Geiger counter. We collected the decay data for the shielded silver and then fitted it with Eq. (8). Looking at the raw data, the short half-life decay appeared much more prominently than in the measurements with the unshielded silver. It appeared that the cadmium shield may have preferentially blocked the activation of the silver isotope associated with the longer decay time (Ag108). Analyzing the data, we found that the

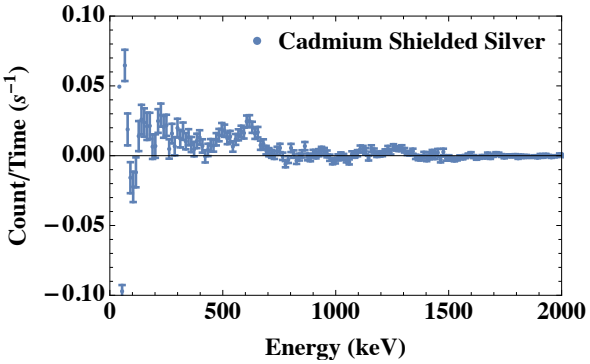

FIG. 9. The measurement of the silver shielded by Cadmium. It looks close to the background.

ratio of the coefficients, N_2/N_1, before the two exponential functions for our shielded silver model was different from the unshielded silver model:

$$\begin{aligned} \text{Silver: } \frac{N_2}{N_1} &= 0.486 \pm 0.041 \\ \text{Silver + Cadmium: } \frac{N_2}{N_1} &= 0.227 \pm 0.020 \end{aligned} \tag{10}$$

where N_1 is the initial number of particles for the short half-life mode (Ag110) and N_2 refers to the long one (Ag108). This means that the shielding effect reduced the long half-life mode activation more than the short one. This also confirms why we see no peaks in the cadmium shielded silver energy spectrum. Since the short mode decays so fast, it is difficult to see its peak in the energy spectrum. Therefore, we can conclude that the cadmium shield blocked the irradiation of Silver-107 (preventing it from becoming Ag-108), while having minimal effect on Silver-109 (allowing it to become Ag-110).

E. Irradiation Time

23 In this section, we investigate the relation between the irradiation time of a sample and its initial count. The initial count refers to the number of activated particles when the sample was removed from the neutron moderator. To obtain the initial count, we maintained a constant time of 15 seconds from when the sample was removed from the moderator until we began counting events with the detector. Then we fit an exponential decay model to our data, where we assigned the beginning time of the model to $t = 15$. From here, we could follow our fitting curve backwards to $t = 0$ to find the probable initial count of irradiated particle in our sample. Due to time constraints we used silver (using the same sample each time after waiting for it to completely decay between trials) as our only test element and ranged the irradiation time from 2 seconds to 60 seconds. These quick trials allowed us to test the irradiation time primarily for the shorter half-life mode of silver. The result is shown in

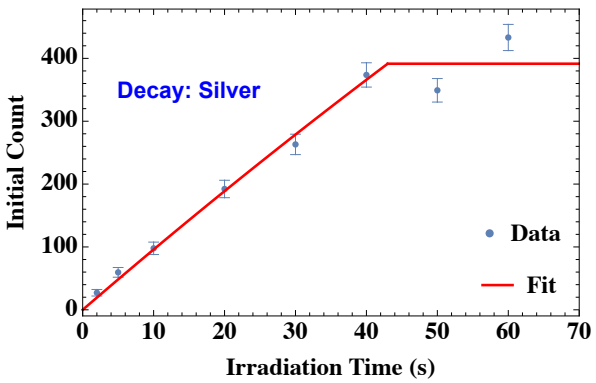

FIG. 10. The relation between the initial count of irradiated silver and its irradiation time. We fitted the data with Eq. (11). The parameter $b \approx 0.0032$ is so small that the curve looks like a linear function [a].

[a] Unfortunately we don't have enough data for the irradiation time, so it is a bit overfitting with Eq. (11)

Fig. 10. Suggested by Eq. (7), we fitted the data using the following form

$$N_0 = a * (e^{-bT} - 1)\Theta(T_0 - T) + c\Theta(T - T_0) \tag{11}$$

Before reaching the saturation point around 43 seconds, the initial count grows exponentially with irradiation time.

IV. CONCLUSION

24 In this paper, we present the measurements of half-lives and energy spectra for several activated metal foil samples. Using the Geiger counter, we captured the decay modes of aluminum, copper, silver and indium, and determined their half-lives, which are in good agreement with the accepted values. The sodium iodide detector allowed us to measure their gamma spectrum and locate the energy peaks. In particle, we find four peaks for the indium and one peak for each of the other samples. Using their identified properties, we attempted to identify two unknown samples. We showed that with reliable data from the unknown samples and comparison with experimental results, it was certainly possible to identify these elements. We also showed the shielding properties of cadmium, in which it blocked one of silver's decay modes, leading to a smaller ratio of the initial counts N_2/N_1. Finally, we show that the initial count of silver grows exponentially with irradiation time until the counts appear to stabilize after 40 seconds.

V. ACKNOWLEDGEMENTS

The authors thank Jenny Hoffman, Matteo Mitrano, Joe Peidle and Jieping Fang for all the help learning how

to use the equipment, providing access to the neutron moderator and guiding us along this experiment. We also thank Jenny Hoffman for very useful comments on the draft version of this report. All the data analyses were completed using `Mathematica 12` and a built-in package `ErrorBarPlots`. For the paper composition, Max completed most of the introduction section and the experimental procedure writeup. Xiaoyuan was primarily responsible for the data analysis portions and their corresponding sections. That being said, this was a collaborative effort and we assisted each other with all elements of the report.

[1] R. Mould, *A Century of X-Rays and Radioactivity in Medicine: With Emphasis on Photographic Records of the Early Years* (CRC Press, 2018).
[2] H. Becquerel, Sur les radiations émises par phosphorescence, Comptes rendus de 1'Academie des Sciences, Paris **122**, 420 (1896).
[3] W. D. Loveland, D. J. Morrissey, and G. T. Seaborg, *Modern Nuclear Chemistry* (New York: John Wiley & Sons, Incorporated, 2017).
[4] S. B. Patel, *Nuclear physics: an introduction* (New Age International, 1991).
[5] Radioactive decay, https://en.wikipedia.org/wiki/Radioactive_decay.
[6] Neutron activation, https://en.wikipedia.org/wiki/Neutron_activation.
[7] Neutron cross section, https://en.wikipedia.org/wiki/Neutron_cross_section.
[8] Gamma spectroscopy, https://en.wikipedia.org/wiki/Gamma_spectroscopy#Sodium_iodide-based_detectors.
[9] M. Wrzesien, L. Albiniak, and H. Al-Hameed, Mts-6 detectors calibration by using 239pu-be neutron source, Medycyna Pracy **68 (6)**, 705 (2017).
[10] B1 induced radioactivity, https://wiki.harvard.edu/confluence/pages/viewpage.action?spaceKey=APL&title=B1.+Induced+Radioactivity#B1.InducedRadioactivity-footnote_1.
[11] R. Lemmerman, engOperation of the geiger counter tube and its associated equipment, The American biology teacher **27**, 435 (1965).
[12] R. B. Firestone and C. M. Baglin, *Table of isotopes*, 8th ed. (Wiley, New York, 1998).
[13] N. Balakrishnan, N. L. Johnson, and S. Kotz, *Continuous univariate distributions* (1994).
[14] W. Feller, V. Feller, and K. M. R. Collection, *An Introduction to Probability Theory and Its Applications*, An Introduction to Probability Theory and Its Applications No. v. 1-2 (Wiley, 1957).
[15] One can also average each data point with several measurements and extract the error from the curve fitting. Since these two methods aim at reducing the statistical errors, they are equivalent.
[16] We tried dropping the first 30 points to fit the background data, but an exponential fitting did not align with the data. Then, going back to the Laurent series, we still needed up to the x^{-4} term. Therefore, we decided it was best to keep the background fitting slightly over-fit, but at least more accurate to our data.

APPENDIX

1. Calibration of the Geiger Counter

25 The equipment required for our Geiger counter measurements was detailed in section II A. However, before measuring the radioactive events per time of our metal foil samples, we had to calibrate our Geiger counter to ensure our MCS received a relevant signal, and to ensure we were applying the ideal voltage to receive a strong signal, but not apply a too high voltage that could damage the equipment or result in excessive dark counts. For our calibration sample, we used Barium-133 which has a long half-life with similar activity to our metal foil samples. First, we connected the Geiger counter directly to an oscilloscope and inserted Barium-133 into the Geiger counter. Once we were able to register pulses, we added the amplifier in series. We then adjusted the amplifier in order to increase the signal to about 1 Volt on the oscilloscope. Next we connected the amplifier to the single channel analyzer to convert to logic pulses. Because we registered at a safe signal voltage (< 5V) for the equipment, we connected our apparatus to the MSC LabView Program. We used the program to record the total counts per 100 seconds at voltages (referring to the high voltages passed directly into the Geiger counter) ranging from 0 to 600 Volts. As expected, our results registered at 0 counts per 100 seconds, until suddenly and rapidly increasing to around 1000 counts per 100 seconds near 500 Volts as seen in Fig 11. The optimal voltage for our experiment was the lowest voltage such that we still received a strong signal. This ensured that we would register many radioactive events, yet not damage the equipment with constant high voltage exceeding the limit of 600V. Therefore, after calibration, we selected a voltage of 510V to use for our Geiger counter experiments.

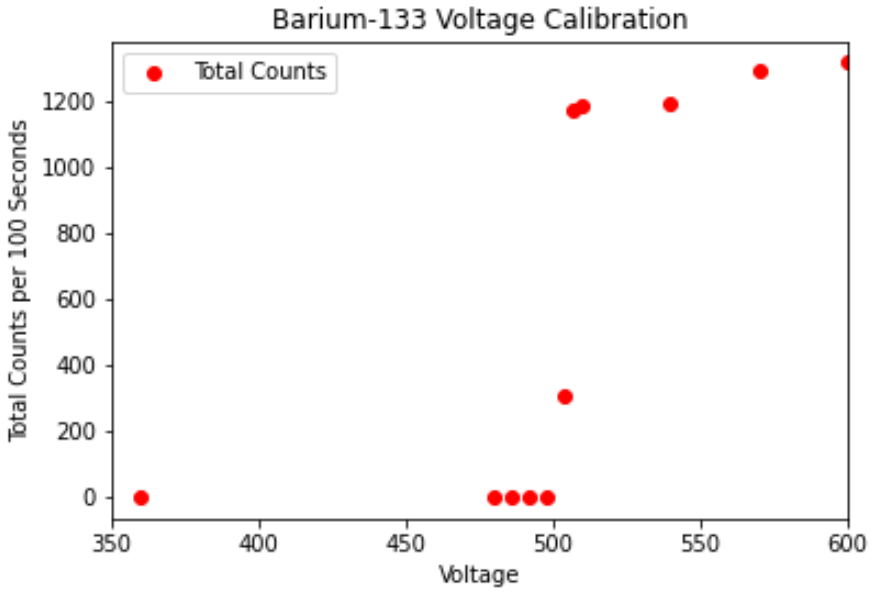

FIG. 11. We took measurements of total counts per 100 seconds for voltages up to 600V. For low voltages, we sporadically took measurements at wide intervals until we found the exponential rise around 500V. Once we determined the general range of the plateau, we took measurements at 6V intervals to characterize the steep curve. We chose the beginning of the plateau for our experimental voltage value (510 Volts) in order to optimize the amount of counts while minimizing stress on equipment.

2. Calibration of the Sodium Iodide Detector

26 In order to calibrate the sodium-iodide detector, we had to first ensure the output signal was at an adequate voltage. After passing the high voltage through the detector, we connected the detector to the amplifier. Using Barium-133 as our initial voltage calibration sample, we adjusted the amplification until the output signal registered around 10 Volts on the oscilloscope. Once this was complete, we connected the detector from the amplifier to the multiple channel analyzer (MCA).

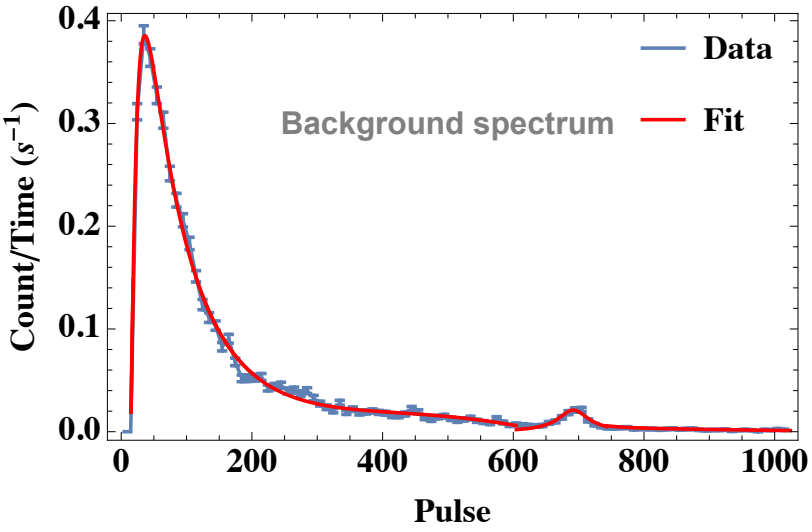

FIG. 12. The background spectrum of the Sodium iodide detector. The blue points are from experiment data with error estimated by Poisson distribution. We bin the data into groups of 10 pulses. The red solid line corresponds to our numerical fit.

Before we measured the calibration samples, we needed to record the background spectrum and remove it from our experiment data. To measure it, we ran the MCA for 500.6 seconds without any sample. The resulting spectrum is shown in Fig. 12, where we normalized by counts per time. The peak registered at low energies comes from some background photons, while the peak around 700 pulses corresponds to Potassium-40 that naturally exists in the concrete comprising the walls of our lab.

To avoid large uncertainty when subtracting the background, we needed to parameterize the background spectrum first. The fitting includes three parts: the low energy region (1-620), the Potassium region (600-750) and the linear region (750-1024). The first region is fitted with a Laurent series, and with powers ranging from -4 to 2. The second region matches the Breit–Wigner distribution (or Cauchy–Lorentz distribution) [13, 14], which is widely used to describe peaks in all aspects of physics. The Breit–Wigner distribution is written as

$$f(x; x_0, \gamma) = \frac{1}{\pi\gamma} \frac{\gamma^2}{(x - x_0)^2 + \gamma^2} \tag{12}$$

where x_0 is the location of the peaks of the distribution and γ is called the scale parameter describing the half-width. Finally, the linear region is fitted with a linear function with a small slope. Note that to reduce the error, we bin the data into groups of 10 pulses. The resulting fit for the background function is then summarized as:

$$\begin{aligned} f(x) = &\left(-\frac{33437.30}{x^4} + \frac{13044.70}{x^3} - \frac{1495.42}{x^2} + \frac{56.48}{x} - 0.32 + 7.50 \times 10^{-4} x - 6.10 \times 10^{-7} x^2\right) \Theta\left(\frac{1209}{2} - x\right) \\ &+ \frac{1.05 \times 10^{-2}}{1 + 1.21 \times 10^{-3}(x - 691.81)^2} \left[\Theta\left(x - \frac{1209}{2}\right) + \Theta\left(\frac{1487}{2} - x\right)\right] + \left(9.24 \times 10^{-3} - 8.02 \times 10^{-6} x\right) \Theta\left(x - \frac{1487}{2}\right) \end{aligned} \tag{13}$$

This may be a little of an over-fitting, however it is difficult to fit the entire background (specifically the low energy region) with any fewer parameters [16]. The comparison between Eq. (13) and the data is also shown in Fig. 12. The fit and the background data are in good agreement apart from the $x \to 0$ region.

Then we collected data for three separate test samples: Americium-241, Barium-133 and Cobalt-60. The energy spectra for these three samples from the MCA are shown in Fig. 13. In these figures, we subtract the background fit function, Eq. (13), and use the Breit–Wigner distribution to find the positions of the peaks.

From the standard gamma spectrum, we know the positions of the peaks in keV as shown in Table V. By identifying the peaks for each sample, we can find the correspondence between the energy of radiation and the signal channels in the MCA. Thus, the energy value, E, of each channel value, V, is given by the function:

$$E = 16.48 + 2.04V(\text{keV}) \tag{14}$$

which is shown in Fig. 14. Using this relation, we can determine the energy of peaks in the activated samples.

Calibration Sample	Peak Position (keV)
Americium-241	59.7
Barium-133	81.0
	356.0
Cobalt 60	1173.0
	1332.0

TABLE V. The literature values of the peak positions [12] for the calibration samples.

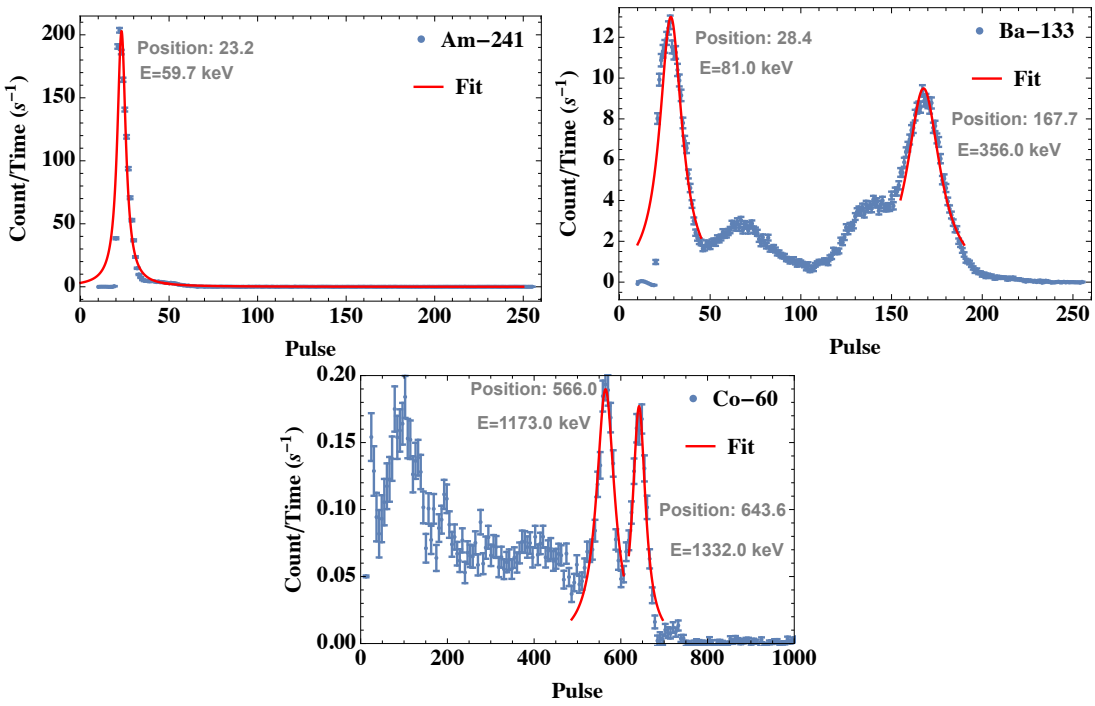

FIG. 13. We measured the energy spectra of Americium-241, Barium-133 and Cobalt-60 using the sodium iodide detector and MCA. We bin the data by 6. The value of E in the figures refers to the energy of the peak determined by Eq. (14). The first two figures have different ranges since there are no peaks in the large pulse region.

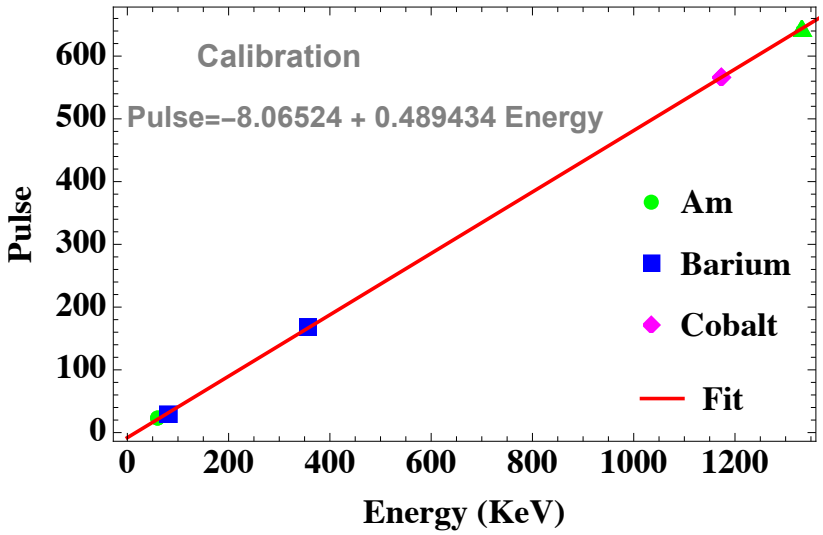

FIG. 14. The relation between the pulse and the energy of our calibration samples with the peak energies obtained from the literature. Note that solving this equation for energy results in Eq. (14), $E = 16.48 + 2.04V(\text{keV})$.